Available online at www.sciencedirect.com
SCIENCE DIRECT®
Journal of Applied Geophysics 54 (2003) 347–367
JOURNAL OF APPLIED GEOPHYSICS
www.elsevier.com/locate/jappgeo

Practical VTI approximations: a systematic anatomy

Paul J. Fowler*

WesternGeco, 1625 Broadway, Suite 1300, Denver, CO 80202, USA

Abstract

Transverse isotropy (TI) with a vertical symmetry axis (VTI) often provides an appropriate earth model for prestack imaging of steep-dip reflection seismic data. Exact P-wave and SV-wave phase velocities in VTI media are described by complicated equations requiring four independent parameters. Estimating appropriate multiparameter earth models can be difficult and time-consuming, so it is often useful to replace the exact VTI equations with simpler approximations requiring fewer parameters. The accuracy limits of different previously published VTI approximations are not always clear, nor is it always obvious how these different approximations relate to each other. Here I present a systematic framework for deriving a variety of useful VTI approximations. I develop first a sequence of well-defined approximations to the exact P-wave and SV-wave phase velocities. In doing so, I show how the useful but physically questionable heuristic of setting shear velocities identically to zero can be replaced with a more precise and quantifiable approximation. The key here to deriving accurate approximations is to replace the stiffness a_{13} with an appropriate factorization in terms of velocity parameters. Two different specific parameter choices lead to the P-wave approximations of Alkhalifah (Geophysics 63 (1998) 623) and Schoenberg and de Hoop (Geophysics 65 (2000) 919), but there are actually an infinite number of reasonable parametrizations possible. Further approximations then lead to a variety of other useful phase velocity expressions, including those of Thomsen (Geophysics 51 (1986) 1954), Dellinger et al. (Journal of Seismic Exploration 2 (1993) 23), Harlan (Stanford Exploration Project Report 89 (1995) 145), and Stopin (Stopin, A., 2001. Comparison of $v(\theta)$ equations in TI medium. 9th International Workshop on Seismic Anisotropy). Each P-wave phase velocity approximation derived this way can be paired naturally with a corresponding SV-wave approximation. Each P-wave or SV-wave phase velocity approximation can then be converted into an equivalent dispersion relation in terms of horizontal and vertical slownesses. A simple heuristic substitution also allows each phase velocity approximation to be converted into an explicit group velocity approximation. From these, in turn, travel time or moveout approximations can also be derived. The group velocity and travel time approximations derived this way include ones previously used by Byun et al. (Geophysics 54 (1989) 1564), Dellinger et al. (Journal of Seismic Exploration 2 (1993) 23), Tsvankin and Thomsen (Geophysics 59 (1994) 1290), Harlan (89 (1995) 145), and Zhang and Uren (Zhang, F. and Uren, N., 2001. Approximate explicit ray velocity functions and travel times for P-waves in TI media. 71st Annual International Meeting, Society of Exploration Geophysicists, Expanded Abstracts, 106–109).

Keywords: Seismic waves; Seismic exploration; Anisotropy; Approximation; Phase velocity; Group velocity

* Tel.: +1-303-389-4416; fax: +1-303-595-0677.
E-mail address: pfowler1@westerngeco.com (P.J. Fowler).

0926-9851/$ - see front matter © 2003 Elsevier B.V. All rights reserved.
doi:10.1016/j.jappgeo.2002.12.002

1. Introduction

Transverse isotropy (TI) often provides a more accurate model of wave propagation than does simple isotropy for characterizing surface seismic reflection data. However, from conventional surface data, it is sometimes a challenge to determine good subsurface velocities for even a simple one-parameter (isotropic, constant density) model of wave propagation, let alone the more complicated model needed for full description of waves in TI media. Complete specification of a TI medium requires defining seven parameters at every subsurface location, namely, five stiffnesses and two angles specifying the symmetry axis orientation. Fortunately, modeling the subsurface by transverse isotropy with a vertical axis of symmetry (VTI) is often adequate for imaging or inverting surface seismic data. This eliminates the two angles as required parameters.

For VTI materials, the dependence of SH-wave phase velocity v_{SH} on phase angle θ is given by

$$v_{SH}^2(\theta) = a_{66}\sin^2\theta + a_{44}\cos^2\theta, \tag{1}$$

where the a_{ij} coefficients are density normalized elements of the material stiffness tensor, that is, $a_{ij} \equiv c_{ij}/\rho$, with c_{ij} the stiffnesses and ρ the density. (All important symbolic notation used here is summarized in Table 1 for reference.) Normalizing like this allows specifying phase velocities without introducing the density as an additional explicit parameter. The dependence of P-wave and SV-wave phase velocities are given by the considerably more complicated relationship

$$2v_{[P,SV]}^2(\theta) = a_{11}\sin^2\theta + a_{33}\cos^2\theta + a_{44} \pm\sqrt{[(a_{11}-a_{44})\sin^2\theta-(a_{33}-a_{44})\cos^2\theta]^2+(a_{13}+a_{44})^2\sin^2 2\theta}, \tag{2}$$

where the plus sign on the radical corresponds to P waves, and the minus sign to SV waves (Michelena, 1993, after Auld, 1990).

The SH-wave phase velocity equation (Eq. (1)) is a simple two-parameter elliptical relation that usually needs no further approximation. However, Eq. (2) for P-wave and SV-wave velocities is complicated in form, and still depends on specification of four independent parameters at every subsurface location.

Table 1
Glossary of symbolic notation

θ	Phase angle	δ	Dimensionless anisotropy parameter
ϕ	Group angle	ϵ	Dimensionless anisotropy parameter
$v_P(\theta)$	P-wave phase velocity	η	Dimensionless anisotropy parameter
$v_{SV}(\theta)$	SV-wave phase velocity	σ	Dimensionless anisotropy parameter
$v_{SH}(\theta)$	SH-wave phase velocity	$v_{pe}(\theta)$	Elliptic part of P-wave phase velocity
$V_P(\phi)$	P-wave group velocity	$V_{pe}(\phi)$	Elliptic part of P-wave group velocity
$V_{SV}(\phi)$	SV-wave group velocity	t_P	P-wave travel time
$V_{SH}(\phi)$	SH-wave group velocity	t_{SV}	SV-wave travel time
a_{ij}	Density-normalized stiffnesses	t_{pe}	Elliptic part of P-wave travel time
v_{pz}	P-wave vertical velocity	t_{sc}	Circular part of SV-wave travel time
v_{px}	P-wave horizontal velocity	x	Horizontal distance
v_{pn}	P-wave NMO velocity	z	Vertical distance
v_{sz}	SV-wave vertical velocity	τ_P	Vertical P-wave travel time
v_{sx}	SV-wave horizontal velocity	v_{p1}	First trial P-wave phase velocity
v_{sn}	SV-wave NMO velocity	v_{p2}	Second trial P-wave phase velocity
p	Horizontal phase slowness	v_{pr}	Reference P-wave phase velocity
q	Vertical phase slowness	r	Normalized vertical phase slowness

In practice, one can often use approximations to Eq. (2) that are simpler in form or lessen the number of independent parameters needed.

Gaiser (1989) and Schoenberg and de Hoop (2000) have derived approximations that simplify the form of Eq. (2), but still retain all four parameters. Several other authors, including Muir and Dellinger (1985), Thomsen (1986), Dellinger et al. (1993), Harlan (1995), Alkhalifah (1998), Zhang and Uren (2001), and Stopin (2001) have published approximations that require only three parameters to define the P-wave phase or group velocity. Schoenberg and de Hoop (2000) also discuss three-parameter approximations, as well as the previously mentioned four-parameter approximations. Because parameter estimation is often one of the most difficult aspects of seismic

imaging, I focus here primarily on approximations like these latter ones that need at most three parameters for P-wave imaging.

Anisotropic approximations can be specified as explicit formulas for the phase velocity as a function of phase angle, or equivalently, as dispersion relations in terms of horizontal and vertical phase velocities. They can also be specified as formulas for the group velocity as a function of group angle, or as travel time or moveout equations. All these forms have been used previously by various authors. Here I develop approximations first in terms of phase velocity functions, but for comparison with other papers and also for practical applications, I also show how to derive corresponding dispersion relations, group velocity equations, and travel time equations.

2. VTI parametrizations and useful identities

Before examining VTI approximations, I summarize here some of the notation used. Three of density-normalized stiffnesses in Eq. (2) have simple interpretations in terms of measurable velocities:

$$a_{11} = v_{px}^2 \tag{3}$$

$$a_{33} = v_{pz}^2 \tag{4}$$

$$a_{44} = v_{sz}^2 = v_{sx}^2, \tag{5}$$

where v_{pz} is the vertical P-wave velocity, v_{px} is the horizontal P-wave velocity, and v_{sz} is the vertical SV-wave velocity, which for VTI will always equal the horizontal SV-wave velocity v_{sx}. The fourth normalized stiffness, a_{13}, also has dimensional units of velocity squared, but is not so easily interpreted.

Thomsen (1986) introduced the dimensionless parameters ε and δ for describing VTI. They are defined in terms of the stiffnesses by

$$\epsilon = \frac{a_{11} - a_{33}}{2a_{33}} \tag{6}$$

$$\delta = \frac{(a_{13} + a_{44})^2 - (a_{33} - a_{44})^2}{2a_{33}(a_{33} - a_{44})}. \tag{7}$$

The Thomsen parameter ϵ relates the vertical P-wave velocity v_{pz} to the horizontal P-wave velocity v_{px} via

$$v_{px}^2 = (1 + 2\epsilon)v_{pz}^2. \tag{8}$$

Similarly, the Thomsen parameter δ relates v_{pz} to v_{pn}, the paraxial curvature of the P wave front around the vertical axis, or equivalently, the small-offset P-wave normal moveout velocity, via

$$v_{pn}^2 = (1 + 2\delta)v_{pz}^2. \tag{9}$$

Alkhalifah and Tsvankin (1995) introduced another useful dimensionless parameter η, defined as

$$\eta = \frac{\epsilon - \delta}{1 + 2\delta}, \tag{10}$$

that links v_{px} and v_{pn} via

$$v_{px}^2 = (1 + 2\eta)v_{pn}^2. \tag{11}$$

A corresponding vertical shear NMO velocity parameter v_{sn} can also be defined (Thomsen, 1986) as

$$v_{sn}^2 = a_{33} - \frac{(a_{13} + a_{44})^2}{a_{11} - a_{44}} \tag{12}$$

$$= (1 + 2\sigma)v_{sz}^2, \tag{13}$$

where the parameter σ for SV waves is defined by

$$\sigma = \frac{(a_{33} - a_{44})(a_{11} - a_{44}) - (a_{13} + a_{44})^2}{2a_{44}(a_{11} - a_{44})} \tag{14}$$

$$= \frac{v_{pz}^2}{v_{sz}^2}(\epsilon - \delta). \tag{15}$$

(Tsvankin and Thomsen, 1994).

The P-wave and SV-wave NMO velocities v_{pn} and v_{sn} are closely related, as shown by the relation

$$v_{pn}^2 - v_{px}^2 = v_{sx}^2 - v_{sn}^2. \tag{16}$$

The P-wave NMO velocity v_{pn} also provides a potential template for replacing the stiffness parameter a_{13}, using the relation

$$(a_{13} + v_{sz}^2)^2 = (v_{pz}^2 - v_{sz}^2)(v_{pn}^2 - v_{sz}^2). \tag{17}$$

Substituting the squared velocities v_{px}^2, v_{pz}^2, and v_{sz}^2 for the stiffnesses a_{11}, a_{33}, and a_{44} in the phase velocity equation (Eq. (2)) converts it into

$$2v_{[P,SV]}^2(\theta) = v_{px}^2\sin^2\theta + v_{pz}^2\cos^2\theta + v_{sz}^2 \pm\sqrt{[(v_{px}^2 - v_{sz}^2)\sin^2\theta - (v_{pz}^2 - v_{sz}^2)\cos^2\theta]^2 + (a_{13} + v_{sz}^2)^2\sin^2 2\theta} \tag{18}$$

$$= v_{px}^2\sin^2\theta + v_{pz}^2\cos^2\theta + v_{sz}^2 \pm\{[(v_{px}^2 - v_{sz}^2)\sin^2\theta + (v_{pz}^2 - v_{sz}^2)\cos^2\theta]^2 + [(a_{13} + v_{sz}^2)^2 - (v_{px}^2 - v_{sz}^2)(v_{pz}^2 - v_{sz}^2)]\sin^2 2\theta\}^{1/2} \tag{19}$$

$$= v_{pe}^2(\theta) + v_{sz}^2 \pm\{[(v_{px}^2 - v_{sz}^2)\sin^2\theta + (v_{pz}^2 - v_{sz}^2)\cos^2\theta]^2 + [(a_{13} + v_{sz}^2)^2 - (v_{px}^2 - v_{sz}^2)(v_{pz}^2 - v_{sz}^2)]\sin^2 2\theta\}^{1/2} \tag{20}$$

$$= v_{pe}^2(\theta) + v_{sz}^2 \pm\{(v_{pe}^2(\theta) - v_{sz}^2)^2 + [(a_{13} + v_{sz}^2)^2 - (v_{px}^2 - v_{sz}^2)(v_{pz}^2 - v_{sz}^2)]\sin^2 2\theta\}^{1/2}. \tag{21}$$

Here the plus sign on the radical again gives the P-wave velocity, the minus sign gives the SV-wave velocity, and I define for convenience the elliptic component of the P-wave velocity $v_{pe}^2(\theta) \equiv v_{px}^2\sin^2\theta + v_{pz}^2\cos^2\theta$.

The P-wave phase velocity is thus a perturbation away from an elliptic velocity function, and the SV-wave phase velocity is similarly a perturbation away from a circular velocity function. These perturbations are of the same magnitude but opposite sign, as shown by the simple relation

$$v_P^2(\theta) - v_{pe}^2(\theta) = v_{sz}^2 - v_{SV}^2(\theta). \tag{22}$$

Although this relation is strictly derived for the exact P-wave and SV-wave velocities, I show later how it can also be used to convert P-wave approximations into formally symmetric SV-wave approximations and vice-versa.

3. Phase velocity approximations

It is sometimes asserted that the P-wave phase velocity in VTI media is only weakly affected by the shear velocity v_{sz}. However, as pointed out by Tsvankin (2001), the truth of this assertion actually depends on the specific parametrization used. The upper plot in Fig. 1 shows $v_P(\theta)$ from Eq. (18). The various curves represent different values of v_{sz} ranging from 1.0 to 2.6 km/s, with $v_{pz} = 4.0$ km/s, $v_{px} = 4.73$ km/s, and $a_{13} = 13.18$ km^2/s^2. Clearly, the P-wave phase velocity here depends strongly on v_{sz}. However, if one uses Eq. (17) to replace a_{13} in Eq. (18) with v_{pn}, this dependence on the value of v_{sz} is nearly eliminated. The lower plot in Fig. 1 shows various curves representing the same range of v_{sz} from 1.0 to 2.6 km/s, with $v_{pz} = 4.0$ km/s and $v_{px} = 4.73$ km/s again, but with $v_{pn} = 3.79$ km/s held

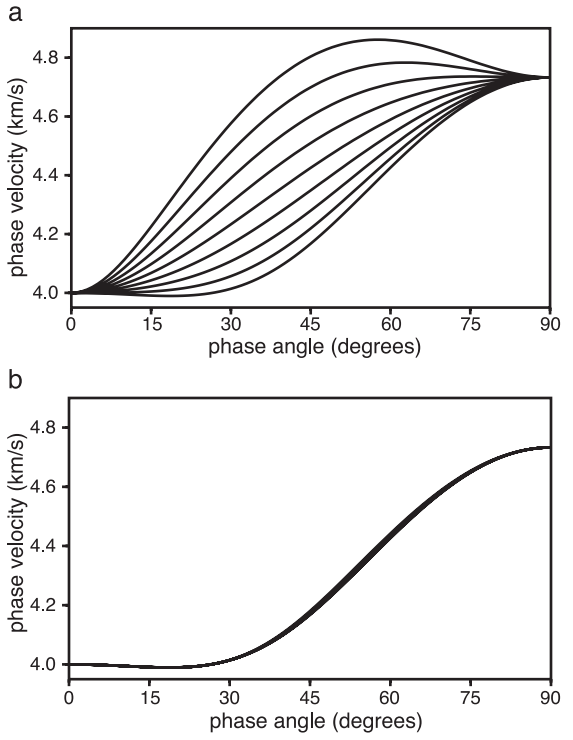

Fig. 1. P-wave phase velocity curves for varying values of v_{sz}. The parameters $v_{pz} = 4$ km/s, $\epsilon = 0.2$, and $\delta = -0.05$ are kept fixed and v_{sz} is allowed to vary from 1.0 to 2.6 km/s. In the upper plot, the P-wave phase velocity is parametrized by the fixed value of $a_{13} = 13.18$ km^2/s^2, whereas in the lower plot a parametrization with a fixed value of $v_{pn} = 3.79$ km/s is used instead. The second parametrization removes nearly all the overt dependence on v_{sz}.

constant now, instead of a fixed value for a_{13}. (The values used for a_{13} and v_{pn} are chosen so that the curves for $v_{sz}=1.0$ km/s are identical in upper and lower figures by design, with both corresponding to setting $\delta=-0.05$.) The curves for different values of v_{sz} are now nearly identical.

The curves in the two plots in Fig. 1 coincide for $v_{sz}=1.0$ km/s by design, but otherwise differ widely between the two figures. The large difference in behavior is caused solely by the change in parametrization. The definition of v_{pn} in Eq. (9) depends on δ, which itself contains both a_{13} and several occurrences of a_{44}, or equivalently, v_{sz}. In effect, the definitions of δ and v_{pn} have isolated those occurrences of v_{sz} that have a significant impact on $v_P(\theta)$ from those that do not.

To derive general P-wave phase velocity approximations that do not depend on v_{sz}, I begin by rewriting Eq. (20) as

$$\begin{aligned}2[v_P^2(\theta)-v_{sz}^2] &= (v_{px}^2-v_{sz}^2)\sin^2\theta+(v_{pz}^2-v_{sz}^2)\cos^2\theta \\ &\quad+\{[(v_{px}^2-v_{sz}^2)\sin^2\theta+(v_{pz}^2-v_{sz}^2)\cos^2\theta]^2 \\ &\quad+[(a_{13}+v_{sz}^2)^2-(v_{px}^2-v_{sz}^2)(v_{pz}^2-v_{sz}^2)]\sin^2 2\theta\}^{1/2}.\end{aligned} \tag{23}$$

I next replace a_{13} using a factorization of the form

$$(a_{13}+v_{sz}^2)^2=(v_{p1}^2-v_{sz}^2)(v_{p2}^2-v_{sz}^2). \tag{24}$$

Here v_{p1}^2 is a general parameter that could take many forms. From Eq. (17), setting $v_{p1}^2=v_{pz}^2$ and $v_{p2}^2=v_{pn}^2$ is one possible choice, but it is not the only one. Once a particular parameter v_{p1}^2 is chosen, the second parameter v_{p2}^2 is then determined as

$$v_{p2}^2=\frac{(a_{13}+v_{sz}^2)^2}{v_{p1}^2-v_{sz}^2}+v_{sz}^2 \tag{25}$$

$$=\frac{(v_{pz}^2-v_{sz}^2)(v_{pn}^2-v_{sz}^2)}{v_{p1}^2-v_{sz}^2}+v_{sz}^2. \tag{26}$$

In terms of this new parametrization, Eq. (23) becomes

$$\begin{aligned}2[v_P^2(\theta)-v_{sz}^2] &= (v_{px}^2-v_{sz}^2)\sin^2\theta+(v_{pz}^2-v_{sz}^2)\cos^2\theta \\ &\quad+\{[(v_{px}^2-v_{sz}^2)\sin^2\theta+(v_{pz}^2-v_{sz}^2)\cos^2\theta]^2 \\ &\quad+[(v_{p1}^2-v_{sz}^2)(v_{p2}^2-v_{sz}^2)-(v_{px}^2-v_{sz}^2) \\ &\quad\times(v_{pz}^2-v_{sz}^2)]\sin^2 2\theta\}^{1/2}\end{aligned} \tag{27}$$

or

$$\begin{aligned}2v_P^2(\theta)&\left[1-\frac{v_{sz}^2}{v_P^2(\theta)}\right] \\ &= v_{px}^2\left(1-\frac{v_{sz}^2}{v_{px}^2}\right)\sin^2\theta+v_{pz}^2\left(1-\frac{v_{sz}^2}{v_{pz}^2}\right)\cos^2\theta \\ &\quad+\left\{\left[v_{px}^2\left(1-\frac{v_{sz}^2}{v_{px}^2}\right)\sin^2\theta+v_{pz}^2\left(1-\frac{v_{sz}^2}{v_{pz}^2}\right)\cos^2\theta\right]^2\right. \\ &\quad+\left[v_{p1}^2v_{p2}^2\left(1-\frac{v_{sz}^2}{v_{p1}^2}\right)\left(1-\frac{v_{sz}^2}{v_{p2}^2}\right)\right. \\ &\quad\left.\left.-v_{px}^2v_{pz}^2\left(1-\frac{v_{sz}^2}{v_{px}^2}\right)\left(1-\frac{v_{sz}^2}{v_{pz}^2}\right)\right]\sin^2 2\theta\right\}^{1/2}.\end{aligned} \tag{28}$$

The purpose of converting the phase velocity equation (Eq. (20)) into the considerably more complicated form of Eq. (28) is to isolate all the explicit occurrences of v_{sz}^2 into factors of the common general form $(1-v_{sz}^2/v_p^2)$. The next step is to pick a constant reference velocity v_{pr}. The value of this reference velocity is somewhat arbitrary, but should usually lie somewhere within the range of $v_P(\theta)$. Using this reference velocity v_{pr}, one can then make the approximations that

$$\left[1-\frac{v_{sz}^2}{v^2(\theta)}\right]\approx\left(1-\frac{v_{sz}^2}{v_{pr}^2}\right) \tag{29}$$

$$\left(1-\frac{v_{sz}^2}{v_{pz}^2}\right)\approx\left(1-\frac{v_{sz}^2}{v_{pr}^2}\right) \tag{30}$$

$$\left(1-\frac{v_{sz}^2}{v_{px}^2}\right)\approx\left(1-\frac{v_{sz}^2}{v_{pr}^2}\right) \tag{31}$$

$$\left(1-\frac{v_{sz}^2}{v_{p1}^2}\right)\approx\left(1-\frac{v_{sz}^2}{v_{pr}^2}\right) \tag{32}$$

$$\left(1-\frac{v_{sz}^2}{v_{p2}^2}\right)\approx\left(1-\frac{v_{sz}^2}{v_{pr}^2}\right). \tag{33}$$

If these approximations are all valid, then all the terms of this form in Eq. (28) can be replaced with similar ones using only the reference velocity, leaving

$$2v_P^2(\theta)\left(1-\frac{v_{sz}^2}{v_{pr}^2}\right) = v_{px}^2\left(1-\frac{v_{sz}^2}{v_{pr}^2}\right)\sin^2\theta + v_{pz}^2\left(1-\frac{v_{sz}^2}{v_{pr}^2}\right)\cos^2\theta + \left\{\left[v_{px}^2\left(1-\frac{v_{sz}^2}{v_{pr}^2}\right)\sin^2\theta + v_{pz}^2\left(1-\frac{v_{sz}^2}{v_{pr}^2}\right)\cos^2\theta\right]^2 + \left[v_{p1}^2 v_{p2}^2\left(1-\frac{v_{sz}^2}{v_{pr}^2}\right)^2 - v_{px}^2 v_{pz}^2\left(1-\frac{v_{sz}^2}{v_{pr}^2}\right)^2\right]\sin^2 2\theta\right\}^{1/2}. \quad (34)$$

All the terms involving the reference velocity now cancel out to give the simpler three-parameter approximation

$$2v_P^2(\theta) = v_{px}^2\sin^2\theta + v_{pz}^2\cos^2\theta + \sqrt{[v_{px}^2\sin^2\theta + v_{pz}^2\cos^2\theta]^2 + (v_{p1}^2 v_{p2}^2 - v_{pz}^2 v_{px}^2)\sin^2 2\theta} \quad (35)$$

$$= v_{pe}^2(\theta) + \sqrt{v_{pe}^4(\theta) + (v_{p1}^2 v_{p2}^2 - v_{pz}^2 v_{px}^2)\sin^2 2\theta} \quad (36)$$

$$= v_{pe}^2(\theta)\left[1 + \sqrt{1 + \frac{(v_{p1}^2 v_{p2}^2 - v_{pz}^2 v_{px}^2)\sin^2 2\theta}{v_{pe}^4(\theta)}}\right]. \quad (37)$$

The simplified approximation in Eq. (35) is formally the same result that one could have obtained by just setting $v_{sz}^2 = 0$ in Eq. (27). However, deriving the result as above demonstrates that one does not actually have to make the unphysical assumption that the shear velocity is identically zero. Both Alkhalifah (1998) and Schoenberg and de Hoop (2000) referred to the step of setting $v_{sz} = 0$ as an "acoustic" approximation, but it might better be called "quasi-acoustic", because some of the influence of a_{44} actually still remains, hidden away now in combination with a_{13} inside the parameter v_{p1}^2.

The reference velocity v_{pr} used above can usually be chosen so that the approximations in Eqs. (29)–(31) will be valid either if the shear velocity is relatively small, or if the P-wave anisotropy is not too great. The smaller the shear velocity, the larger the P-wave anisotropy can become while retaining a specified level of accuracy in the approximation, and likewise, the less the P-wave anisotropy, the larger the shear velocity can be.

The approximations in Eqs. (30) and (31) are usually reasonable if the ellipticity of the phase velocity is not too large. The validity of the approximations in Eqs. (32) and (33) obviously depends on how one chooses the parameter v_{p1}^2. There are an unlimited number of ways to make this choice. In general, one should try to bound v_{p1}^2 so that $v_{pmin}^2 \le v_{p1}^2 \le v_{pmax}^2$ and $v_{pmin}^2 \le v_{p2}^2 \le v_{pmax}^2$, where v_{pmin} and v_{pmax} are the minimum and maximum values of $v_P(\theta)$, respectively. This bound will ensure that Eq. (29) will limit the accuracy of the overall approximation rather than either Eq. (32) or Eq. (33).

A few specific choices for the parameter v_{p1}^2 are of particular interest here. First, setting $v_{p1}^2 = v_{p2}^2 = -a_{13}$ is equivalent to what one would get by skipping the factorization in Eq. (27) and just setting $v_{sz} = 0$ in the original Eq. (23). As was shown in Fig. 1, this is a poor approximation, because $-a_{13}$ usually will not fall within the range of $v_P^2(\theta)$, so I will not consider it further here. Next, one could set $v_{p1}^2 = v_{pz}^2$ and $v_{p2}^2 = v_{pn}^2$. This is equivalent to the approximation used (in somewhat different form) by Alkhalifah (1998). With a bit of algebra, it can also be shown to be equivalent to the approximation used in Eq. (8) of Stopin (2001). Another reasonable choice might be to set $v_{p1}^2 = v_{p2}^2 = a_{13} + 2v_{sz}^2$, as suggested in Schoenberg and de Hoop (2000).Many other choices are also possible. For example, one could set $v_{p1}^2 = v_{px}^2$, or $v_{p1}^2 = v_{pz}v_{px}$, or $v_{p1}^2 = (v_{pz}^2 + v_{px}^2)/2$, or $v_{p1}^{-2} = (v_{pz}^{-2} + v_{px}^{-2})/2$. In each of these cases, v_{p2}^2 is then found from Eq. (25) or Eq. (26). Since each of these choices would usually satisfy the requirement that v_{p1}^2 and v_{p2}^2 lie within the range of $v_P^2(\theta)$ one could expect that they all would lead to reasonable approximations.

Fig. 2 compares these different choices for the parameter v_{p1}^2. The figure has two parts: the first shows P-wave phase velocity over a range of 0° to

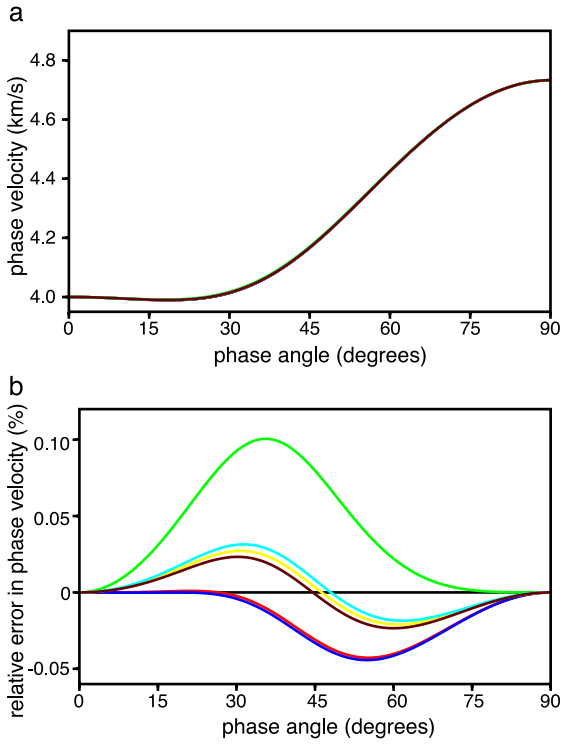

Fig. 2. P-wave phase velocity curves for different choices of the parameter v_{p1}. The upper plot shows the phase velocity curves, and the second one shows the errors relative to the exact phase velocity. The black line is the exact phase velocity for $v_{pz}=4$ km/s, $v_{sz}=1$ km/s, $\epsilon=0.2$, and $\delta=-0.05$. The colored lines are different choices of v_{p1}; the specific values are detailed in the main text. For this example, all the v_{p1} choices produce excellent approximations, and the different lines in the top plot are barely distinguishable.

90°, and the second shows the relative errors of each approximation compared to the exact P-wave phase velocity. The curves are all computed for $v_{pz}=4$ km/s, $v_{sz}=1$ km/s, $\epsilon=0.2$, and $\delta=-0.05$, as are all similar plots for the rest of this paper. The black curve represents the exact P-wave phase velocity, so in the relative error plot it is a horizontal line at value zero. The first approximation ($v_{p1}^2=v_{pz}^2$) is the red line, the second approximation ($v_{p1}^2=a_{13}+2v_{sz}^2$) is the dark blue line, the third approximation ($v_{p1}^2=v_{px}^2$) is the green line, the fourth approximation ($v_{p1}^2=v_{pz}v_{px}$) is the yellow line, the fifth approximation ($v_{p1}^2=(v_{pz}^2+v_{px}^2)/2$) is light blue line, and the sixth approximation ($v_{p1}^{-2}=(v_{pz}^{-2}+v_{px}^{-2})/2$) is the brown line. All the approximations work very well for this example, so well in fact that the curves in the upper plot are essentially indistinguishable, and all have a maximum relative error of a small fraction of a percent.

Eq. (37) can be approximated further by expanding the square root in a Taylor expansion. Note from Eq. (26) that in the limit of $v_{sz}\downarrow 0$ one gets $v_{p1}^2v_{p2}^2=v_{pz}^2v_{pn}^2$ independent of the particular choice of v_{p1}^2. Thus it should usually be reasonably accurate to expect that $|v_{p1}^2v_{p2}^2-v_{pz}^2v_{px}^2|\ll v_{pe}^4(\theta)$, so only the first linear term of the Taylor expansion should be needed. The resulting error can be estimated from the standard Taylor expansion error expression if required.

Linearizing Eq. (37) in this manner then gives

$$v_P^2(\theta)=v_{pe}^2(\theta)\left[1+\frac{v_{p1}^2v_{p2}^2-v_{pz}^2v_{px}^2)\sin^2\theta\cos^2\theta}{v_{pe}^4(\theta)}\right] \tag{38}$$

$$=\frac{v_{pz}^4\cos^4\theta+v_{pz}^2v_{px}^2\left(1+\frac{v_{p1}^2v_{p2}^2}{v_{pz}^2v_{px}^2}\right)\sin^2\theta\cos^2\theta+v_{px}^4\sin^4\theta}{v_{pz}^2\cos^2\theta+v_{px}^2\sin^2\theta}. \tag{39}$$

This is now in exactly the general Muir–Dellinger rational fraction form (Muir and Dellinger, 1985; Dellinger et al., 1993). Linearizing the three-parameter P-wave approximation thus gives this rational fraction form independent of the particular choice of the parameter v_{p1}.

The parametrization choice $v_{p1}=v_{pz}$ and $v_{p2}=v_{pn}$ is particularly convenient because v_{pn} has a familiar interpretation as a moveout velocity and can often be measured from surface seismic data. With this choice, the first approximation in Eqs. (36) and (37) becomes

Approximation P1

$$2v_P^2(\theta)=v_{pe}^2(\theta)+\sqrt{v_{pe}^4(\theta)+v_{pz}^2(v_{pn}^2-v_{px}^2)\sin^2 2\theta} \tag{40}$$

$$=v_{pe}^2(\theta)\left[1+\sqrt{1+\frac{v_{pz}^2(v_{pn}^2-v_{px}^2)\sin^2 2\theta}{v_{pe}^4(\theta)}}\right]. \tag{41}$$

This is equivalent to the "empirical approximation" of Stopin (2001), and also corresponds to the dispersion relation approximation used by Alkhalifah (1998).

With the same parameter choice of $v_{p1}=v_{pz}$ the Muir–Dellinger approximation in Eq. (38) simplifies to

Approximation P2

$$v_P^2(\theta)=v_{pe}^2(\theta)+\frac{v_{pz}^2(v_{pn}^2-v_{px}^2)}{v_{pe}^2(\theta)}\sin^2\theta\cos^2\theta. \tag{42}$$

This is equivalent to the specific parametrization used in Dellinger et al. (1993). It is also equivalent to the dispersion relation approximation derived by Klie and Toro (2001).

This approximation can be carried one step further by writing Eq. (42) as

$$v_P^2(\theta)=v_{pe}^2(\theta)\left[1+\frac{v_{pz}^2(v_{pn}^2-v_{px}^2)}{v_{pe}^4(\theta)}\sin^2\theta\cos^2\theta\right]. \tag{43}$$

Taking the square root of both sides and linearizing the resulting radical on the right side then gives

Approximation P3

$$v_P(\theta)=v_{pe}(\theta)+\frac{v_{pz}^2(v_{pn}^2-v_{px}^2)}{2v_{pe}^3(\theta)}\sin^2\theta\cos^2\theta. \tag{44}$$

Another useful approximation can be derived by setting $v_{pe}(\theta)\approx v_{pz}$ in the denominator of the second (anelliptic) term of Eq. (42), yielding

Approximation P4

$$v_P^2(\theta)=v_{pe}^2(\theta)+(v_{pn}^2-v_{px}^2)\sin^2\theta\cos^2\theta \tag{45}$$

$$=v_{pz}^2\cos^2\theta+v_{pn}^2\sin^2\theta\cos^2\theta+v_{px}^2\sin^4\theta. \tag{46}$$

This is the simple form suggested by Harlan (1995), and is also equivalent to the "weak-anisotropy-squared" approximation of Stopin (2001). The nature of the approximation $v_{pe}(\theta)\approx v_{pz}$ suggests that this form is most accurate near vertical, and for media in which the ellipticity ϵ is small. Note that approximation P4 is linear if one uses the squared velocities as material parameters.

Approximation P4 can be linearized one step further just as P2 was, giving

Approximation P5

$$v_P(\theta)=v_{pe}(\theta)+\frac{(v_{pn}^2-v_{px}^2)}{2v_{pe}(\theta)}\sin^2\theta\cos^2\theta. \tag{47}$$

Many slightly different perturbations in the anelliptic term in approximation P2 can also lead to other reasonable approximations. One possibility is to modify the $v_{pe}^2(\theta)$ factor in the denominator by replacing v_{px}^2 with (v_{pn}^4/v_{px}^2) to get

Approximation P6

$$v_P^2(\theta)=v_{pe}^2(\theta)+\frac{v_{pz}^2(v_{pn}^2-v_{px}^2)}{v_{pz}^2\cos^2\theta+\frac{v_{pn}^4}{v_{px}^2}\sin^2\theta}\sin^2\theta\cos^2\theta. \tag{48}$$

The motivation for this particular approximation is probably not apparent now, but it will be shown later to lead to the moveout approximation used by Tsvankin and Thomsen (1994). Approximation P6 can also again be further linearized, yielding

Approximation P7

$$v_P(\theta)=v_{pe}(\theta)+\frac{v_{pz}^2(v_{pn}^2-v_{px}^2)}{2v_{pe}(\theta)\left[v_{pz}^2\cos^2\theta+\frac{v_{pn}^4}{v_{px}^2}\sin^2\theta\right]}\times\sin^2\theta\cos^2\theta. \tag{49}$$

One can also derive approximations directly from the exact phase velocity expression without suppressing v_{sz} as a parameter. The exact P-wave phase velocity expression from Eq. (21) can be rewritten as

$$2v_P^2(\theta)=v_{pe}^2(\theta)+v_{sz}^2+[v_{pe}^2(\theta)-v_{sz}^2]\times\sqrt{1+\frac{(a_{13}+v_{sz})^2-(v_{pz}^2-v_{sz}^2)(v_{px}^2-v_{sz}^2)}{[v_{pe}^2(\theta)-v_{sz}^2]^2}\sin^2 2\theta}. \tag{50}$$

Linearizing the radical on the right then gives

$$2v_P^2(\theta)=v_{pe}^2(\theta)+v_{sz}^2+[v_{pe}^2(\theta)-v_{sz}^2]\times\left\{1+\frac{(a_{13}+v_{sz})^2-(v_{pz}^2-v_{sz}^2)(v_{px}^2-v_{sz}^2)}{2[v_{pe}^2(\theta)-v_{sz}^2]^2}\sin^2 2\theta\right\}. \tag{51}$$

Using the substitution from Eq. (17) this simplifies to

Approximation P8

$$v_P^2(\theta)=v_{pe}^2(\theta)+\frac{(v_{pz}^2-v_{sz}^2)(v_{pn}^2-v_{px}^2)}{v_{pe}^2(\theta)-v_{sz}^2}\sin^2\theta\cos^2\theta. \tag{52}$$

This can again be linearized one more time to yield.

Approximation P9

$$v_P(\theta) = v_{pe}(\theta) + \frac{(v_{pz}^2 - v_{sz}^2)(v_{pn}^2 - v_{px}^2)}{2v_{pe}(\theta)[v_{pe}^2(\theta) - v_{sz}^2]}\sin^2\theta\cos^2\theta. \tag{53}$$

Approximations P8 and P9 are very similar to approximations P2 and P3, but without the simplifying elimination of the extra v_{sz} parameter.

All of the preceding approximations take the form of anelliptic perturbations away from the elliptical velocity $v_{pe}(\theta)$ or its square $v_{pe}^2(\theta)$. It is also possible to derive alternative approximations based on other expansions. As an example, approximation P4 in Eq. (46) can be expanded around the vertical velocity v_{pz} instead of the elliptical velocity $v_{pe}(\theta)$, giving

$$v_P^2(\theta) = v_{pz}^2\left[1 + \left(\frac{v_{pn}^2}{v_{pz}^2} - 1\right)\sin^2\theta\cos^2\theta + \left(\frac{v_{px}^2}{v_{pz}^2} - 1\right)\sin^4\theta\right]. \tag{54}$$

Taking the square root of each side and linearizing the resulting radical then gives

Approximation P10

$$v_P(\theta) = v_{pz}\left[1 + \frac{1}{2}\left(\frac{v_{pn}^2}{v_{pz}^2} - 1\right)\sin^2\theta\cos^2\theta + \frac{1}{2}\left(\frac{v_{px}^2}{v_{pz}^2} - 1\right)\sin^4\theta\right] \tag{55}$$

$$= v_{pz}\left(1 + \cos^2\theta + \frac{v_{pn}^2}{v_{pz}^2}\sin^2\theta\cos^2\theta + \frac{v_{px}^2}{v_{pz}^2}\sin^4\theta\right) \tag{56}$$

$$= v_{pz}\left(1 + \delta\sin^2\theta\cos^2\theta + \epsilon\sin^4\theta\right). \tag{57}$$

This is now the approximation suggested by Thomsen (1986). Unfortunately, expanding around the vertical velocity v_{pz} has made approximation P10 no longer fit the horizontal P-wave velocity v_{px} correctly, which makes wide angle propagation less accurate.

All these various P-wave phase velocity approximations are summarized in Table 2. Corresponding approximations can be developed expressing the SV-wave phase velocity as perturbations away from a circular velocity function. These SV-wave approximations are also summarized in Table 2. In deriving these SV-wave phase velocity approximations, I used Eq. (22) to associate a matching $v_{SV}^2(\theta)$ approximation with each of the $v_P^2(\theta)$ approximations P1, P2, P4, P6, and P8. Approximations SV2, SV4, SV6, and SV8 can in turn each be further linearized to get the other $v_{SV}(\theta)$ approximations SV3, SV5, SV7, and SV9. For convenience in comparing with other published approximations, and for later use in deriving group velocity approximations, I have also used Eq. (16) to replace the factors of $v_{pn}^2 - v_{px}^2$ with equivalent factors of $v_{sz}^2 - v_{sn}^2$ in all the SV-wave phase velocity approximations.

Several features of these SV-wave phase velocity approximations are worth noting. Approximation SV1 is equivalent to the "empirical approximation" of Stopin (2001). Similarly, approximation SV4 is equivalent to the "weak anisotropy squared" SV approximation of Stopin (2001). Approximation SV4 has other properties worth noting. It is linear in the squared velocity parameters, and requires only the two shear wave velocities v_{sn} and v_{sz} as parameters. Approximation SV4 can also be cast into the equivalent rational fraction form

$$v_{SV}^2(\theta) = \frac{v_{sx}^4\sin^4\theta + v_{sz}^2 v_{sx}^2\left(1 + \frac{v_{sn}^2}{v_{sx}^2}\right)\sin^2\theta\cos^2\theta + v_{sz}^4\cos^4\theta}{v_{sz}^2\cos^2\theta + v_{sx}^2\sin^2\theta}, \tag{58}$$

in which form it can be recognized as also equivalent to the SV-wave phase velocity approximation of Dellinger et al. (1993). Approximation SV5, the result of further linearization of approximation SV4, can also be written as

$$v_{SV}(\theta) = v_{sz}(1 + \sigma\sin^2\theta\cos^2\theta), \tag{59}$$

which is just the SV-wave approximation introduced by Thomsen (1986). Because the horizontal and vertical velocities are the same for SV waves, unlike the P-wave case, there is now no need to distinguish a separate expansion around vertical

Table 2
Phase velocity approximations

P1	$2v_P^2(\theta) = v_{pe}(\theta) + \sqrt{v_{pe}^4(\theta) + v_{pz}^2(v_{pn}^2 - v_{px}^2)\sin^2 2\theta}$
P2	$v_P^2(\theta) = v_{pe}^2(\theta) + \frac{v_{pz}^2(v_{pn}^2 - v_{px}^2)}{v_{pe}^2(\theta)}\sin^2\theta\cos^2\theta$
P3	$v_P(\theta) = v_{pe}(\theta) + \frac{v_{pz}^2(v_{pn}^2 - v_{px}^2)}{2v_{pe}^3(\theta)}\sin^2\theta\cos^2\theta$
P4	$v_P^2(\theta) = v_{pe}^2(\theta) + (v_{pn}^2 - v_{px}^2)\sin^2\theta\cos^2\theta$
P5	$v_P(\theta) = v_{pe}(\theta) + \frac{(v_{pn}^2 - v_{px}^2)}{2v_{pe}(\theta)}\sin^2\theta\cos^2\theta$
P6	$v_P^2(\theta) = v_{pe}^2(\theta) + \frac{v_{pz}^2(v_{pn}^2 - v_{px}^2)}{v_{pz}^2\cos^2\theta + v_{pn}^4 v_{px}^{-2}\sin^2\theta}\sin^2\theta\cos^2\theta$
P7	$v_P(\theta) = v_{pe}(\theta) + \frac{v_{pz}^2(v_{pn}^2 - v_{px}^2)}{2v_{pe}(\theta)(v_{pz}^2\cos^2\theta + v_{pn}^4 v_{px}^{-2}\sin^2\theta)} \times \sin^2\theta\cos^2\theta$
P8	$v_P^2(\theta) = v_{pe}^2(\theta) + \frac{(v_{pz}^2 - v_{sz}^2)(v_{pn}^2 - v_{px}^2)}{v_{pe}^2(\theta) - v_{sz}^2}\sin^2\theta\cos^2\theta$
P9	$v_P(\theta) = v_{pe}(\theta) + \frac{(v_{pz}^2 - v_{sz}^2)(v_{pn}^2 - v_{px}^2)}{2v_{pe}(\theta)[v_{pe}^2(\theta) - v_{sz}^2]}\sin^2\theta\cos^2\theta$
P10	$2v_P(\theta) = v_{pz}\left(1 + \cos^2\theta + \frac{v_{pn}^2}{v_{pz}^2}\sin^2\theta\cos^2\theta + \frac{v_{px}^2}{v_{pz}^2}\sin^4\theta\right)$
SV1	$2v_{SV}^2(\theta) = 2v_{sz}^2 + v_{pe}^2(\theta) - \sqrt{v_{pe}^4(\theta) + v_{pz}^2(v_{sz}^2 - v_{sn}^2)\sin^2 2\theta}$
SV2	$v_{SV}^2(\theta) = v_{sz}^2 - \frac{v_{pz}^2(v_{sz}^2 - v_{sn}^2)}{v_{pe}^2(\theta)}\sin^2\theta\cos^2\theta$
SV3	$v_{SV}(\theta) = v_{sz} - \frac{v_{pz}^2(v_{sz}^2 - v_{sn}^2)}{2v_{sz}v_{pe}^2(\theta)}\sin^2\theta\cos^2\theta$
SV4	$v_{SV}^2(\theta) = v_{sz}^2 - (v_{sz}^2 - v_{sn}^2)\sin^2\theta\cos^2\theta$

Table 2 (*continued*)

SV5	$v_{SV}(\theta) = v_{sz} - \frac{v_{sz}^2 - v_{sn}^2}{v_{sz}}\sin^2\theta\cos^2\theta$
SV6	$v_{SV}^2(\theta) = v_{sz}^2(\theta) - \frac{v_{pz}^2(v_{sz}^2 - v_{sn}^2)}{v_{pz}^2\cos^2\theta + v_{pn}^4 v_{px}^{-2}\sin^2\theta} \times \sin^2\theta\cos^2\theta$
SV7	$v_{SV}(\theta) = v_{sz}(\theta) - \frac{v_{pz}^2(v_{sz}^2 - v_{sn}^2)}{2v_{sz}(v_{pz}^2\cos^2\theta + v_{pn}^4 v_{px}^{-2}\sin^2\theta)} \times \sin^2\theta\cos^2\theta$
SV8	$v_{SV}^2(\theta) = v_{sz}^2 - \frac{(v_{pz}^2 - v_{sz}^2)(v_{sz}^2 - v_{sn}^2)}{v_{pe}^2(\theta) - v_{sz}^2}\sin^2\theta\cos^2\theta$
SV9	$v_{SV}(\theta) = v_{sz} - \frac{(v_{pz}^2 - v_{sz}^2)(v_{sz}^2 - v_{sn}^2)}{2v_{sz}[v_{pe}^2(\theta) - v_{sz}^2]}\sin^2\theta\cos^2\theta$

velocity for SV waves as was done to derive approximation P10.

These are of course not the only possible P-wave or SV-wave approximations. Further approximations could be derived by various other modifications of the anelliptic terms. One could also potentially gain greater accuracy by retaining higher order terms in a Taylor, Padé, or similar expansion to replace the various square roots. Some examples of higher order approximations are presented by Gaiser (1989), Dellinger et al. (1993), and Schoenberg and de Hoop (2000).

Fig. 3 compares the different P-wave phase velocity approximations P1 through P10.The model parameters used are again $v_{pz}=4$ km/s, $v_{sz}=1$ km/s, $\epsilon=0.2$, and $\delta=-0.05$. In this figure, there are 11 curves. The solid black line represents the exact P-wave phase velocity, approximation P1 is the black dashed line, P2 is solid red, P3 is dashed red, P4 is solid blue, P5 is dashed blue, P6 is solid green, P7 is dashed green, P8 is solid yellow, P9 is dashed yellow, and P10 is dashed light blue. The upper plot compares the different phase velocity approximations, and the second shows the errors relative to the exact phase velocity. Note, however, that both the patterns of

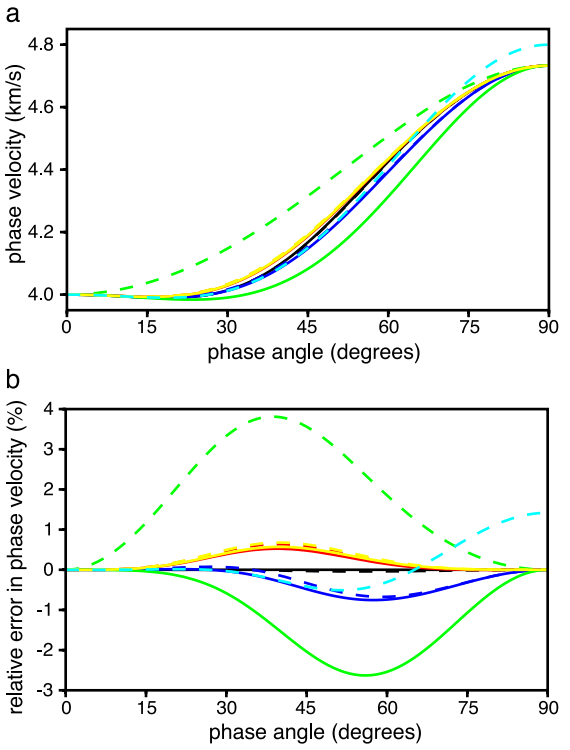

Fig. 3. P-wave phase velocity approximations. The upper plot shows various P-wave phase velocity approximations, and the lower plot shows the relative errors compared to the exact P-wave phase velocity. The black line is the exact P-wave phase velocity for $v_{pz}=4$ km/s, $\epsilon=0.2$, and $\delta=-0.05$, and $v_{sz}=1$ km/s. Approximation P1 is the black dashed line, P2 is solid red, P3 is dashed red, P4 is solid blue, P5 is dashed blue, P6 is solid green, P7 is dashed green, P8 is solid yellow, P9 is dashed yellow, and P10 is dashed light blue.

error and the relative accuracy of different approximations can differ significantly depending on the specific choices of material parameters, so one should be cautious in drawing any strong conclusions about relative merits of different approximations from this single figure.

Fig. 4 similarly compares the different SV-wave phase velocity approximations SV1 through SV10.The model parameters used are the same as for Fig. 3, and two plots again show the different phase velocity approximations and their relative errors. The solid black line again represents the exact SV-wave phase velocity, approximation SV1 is the black dashed line, SV2 is solid red, SV3 is dashed red, SV4 is solid blue, SV5 is dashed blue, SV6 is solid green, SV7 is dashed green, SV8 is solid yellow, and SV9 is dashed yellow. All of the SV-wave phase velocity approximations have relative errors that are large compared with those of the P-wave phase velocity approximations, in part because they are being compared to an exact value that is much smaller in magnitude. Note again, too, that this is only one illustrative example, and the patterns of error and relative accuracies can differ significantly with different choices of material parameters.

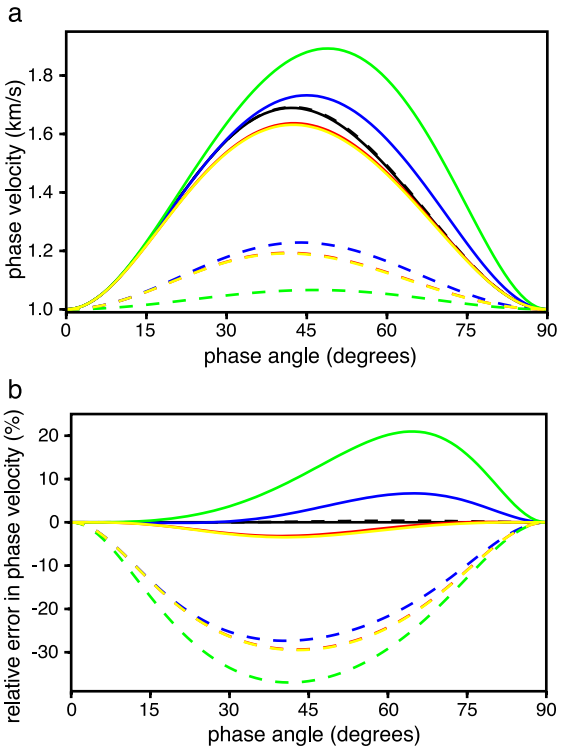

Fig. 4. SV-wave phase velocity approximations. The upper plot shows various SV-wave phase velocity approximations, and the lower plot shows the relative errors compared to the exact SV-wave phase velocity. The black line is the exact SV-wave phase velocity for $v_{pz}=4$ km/s, $\epsilon=0.2$, and $\delta=-0.05$, and $v_{sz}=1$ km/s. Approximation SV1 is the black dashed line, SV2 is solid red, SV3 is dashed red, SV4 is solid blue, SV5 is dashed blue, SV6 is solid green, SV7 is dashed green, SV8 is solid yellow, and SV9 is dashed yellow.

4. Dispersion relation approximations

Imaging methods based on F–K downward extrapolation are more naturally formulated using dispersion relations instead of phase velocity formulas (e.g., Gazdag, 1978, or Stolt, 1978). Dispersion relations can also be used to derive finite-difference extrapolation and imaging approaches (e.g., Claerbout, 1984). The approximations developed so far in this paper express the phase velocity as a function of phase angle. A dispersion relation instead expresses a relationship between the horizontal phase slowness $p=\sin\theta/v(\theta)$ and the vertical phase slowness $q=\cos\theta/v(\theta)$. For application, the phase slownesses can be interpreted in the space-time domain as $p=\mathrm{d}t/\mathrm{d}x$ and $q=\mathrm{d}t/\mathrm{d}z$, converting the dispersion relation into an eikonal equation. Alternatively, the phase slownesses can be interpreted in the Fourier domain as $p=K_x/\omega$ and $q=K_z/\omega$, in which case the dispersion relation describes propagation of plane waves. Each Fourier domain dispersion relation can then further be converted into a partial differential wave equation if desired.

The information contained in a velocity function and in the corresponding dispersion relation is fundamentally the same. Each approximation for phase velocity can be converted into a dispersion relation equation by dividing through by an appropriate power of $v(\theta)$ and making judicious use of the identity $p^2+q^2=1/v^2(\theta)$. Doing so for the exact P-wave and SV-wave phase velocity equation (Eq. (18)) gives the dispersion relation

$$2=(v_{px}^2+v_{sz}^2)p^2+(v_{pz}^2+v_{sz}^2)q^2 \pm\sqrt{[(v_{px}^2-v_{sz}^2)p^2-(v_{pz}^2-v_{sz}^2)q^2]^2+4(a_{13}+v_{sz}^2)^2p^2q^2}, \tag{60}$$

or, expanding all terms into a polynomial equation,

$$v_{px}^2v_{sz}^2p^4+v_{pz}^2v_{sz}^2q^4+[v_{pz}^2v_{px}^2+v_{sz}^4-(a_{13}^2+v_{sz}^2)^2]p^2q^2-(v_{px}^2+v_{sz}^2)p^2-(v_{pz}^2+v_{sz}^2)q^2+1=0. \tag{61}$$

The general quasi-acoustic P-wave phase velocity approximation in Eq. (34) similarly corresponds to the dispersion relation

$$2=v_{px}^2p^2+v_{pz}^2q^2+\sqrt{(v_{px}^2p^2+v_{pz}^2q^2)^2+4(v_{p1}^2v_{p2}^2-v_{pz}^2v_{px}^2)p^2q^2}, \tag{62}$$

or, expanded again into a polynomial equation,

$$v_{px}^2p^2+v_{pz}^2q^2+(v_{p1}^2v_{p2}^2-v_{pz}^2v_{px}^2)p^2q^2-1=0. \tag{63}$$

As one might expect, this is the same result one would get from applying the factorization from Eq. (24) to (61) and then setting $v_{sz}=0$. For the specific choice of $v_{p1}=a_{13}+2v_{sz}^2$, Eq. (63) reduces to Eq. (37) of Schoenberg and de Hoop (2000). The choice instead of $v_{p1}=v_{pz}$ gives

$$v_{px}^2p^2+v_{pz}^2q^2+v_{pz}^2(v_{pn}^2-v_{px}^2)p^2q^2-1=0. \tag{64}$$

This is the dispersion relation corresponding to approximation P1, and also agrees with Eq. (5) of Alkhalifah (1998). Dispersion relations for the other P-wave and SV-wave approximations can be derived similarly and are summarized in Table 3.

For imaging using downward continuation methods, one usually wants to solve for q as a function of p. Each of the dispersion relation approximations can be expanded into a polynomial equation. The exact dispersion relation, and approximations P2, P4, P6, P8, SV1, SV2, SV4, SV6, and SV8, all yield fourth order polynomial equations that contain only even-order powers of p and q, so they can be solved as quadratic equations in the squared variables. Approximations P3, P5, P7, P9, SV3, SV5, SV7, and SV9 give eighth order polynomial equations, and require the solution of full quartic equations in the squared variables. Approximation P1 has the attractive property that it can be solved immediately as a quadratic equation in q to give

$$q(p)=\frac{1}{v_{pz}}\sqrt{\frac{1-v_{px}^2p^2}{1+(v_{pn}^2-v_{px}^2)p^2}}. \tag{65}$$

As pointed out by Alkhalifah (1998), the v_{pz} factors in the P1 dispersion relation of Eq. (64) can always be paired with matching q factors, which allows separation of imaging from depth conversion in laterally

Table 3
Dispersion relation approximations

P1	$2 = v_{px}^2 p^2 + v_{pz}^2 q^2 + \sqrt{(v_{px}^2 p^2 + v_{pz}^2 q^2)^2 + 4v_{pz}^2 (v_{pn}^2 - v_{px}^2) p^2 q^2}$
P2	$1 = v_{px}^2 p^2 + v_{pz}^2 q^2 + \frac{v_{pz}^2 (v_{pn}^2 - v_{px}^2) p^2 q^2}{v_{px}^2 p^2 + v_{pz}^2 q^2}$
P3	$1 = (v_{px}^2 p^2 + v_{pz}^2 q^2)^{1/2} + \frac{v_{pz}^2 (v_{pn}^2 - v_{px}^2) p^2 q^2}{2(v_{px}^2 p^2 + v_{pz}^2 q^2)^{3/2}}$
P4	$1 = v_{px}^2 p^2 + v_{pz}^2 q^2 + \frac{(v_{pn}^2 - v_{px}^2) p^2 q^2}{p^2 + q^2}$
P5	$1 = (v_{px}^2 p^2 + v_{pz}^2 q^2)^{1/2} + \frac{(v_{pn}^2 - v_{px}^2) p^2 q^2}{2(p^2 + q^2)(v_{px}^2 p^2 + v_{pz}^2 q^2)^{1/2}}$
P6	$1 = v_{px}^2 p^2 + v_{pz}^2 q^2 + \frac{v_{pz}^2 (v_{pn}^2 - v_{px}^2) p^2 q^2}{v_{pn}^4 v_{px}^{-2} p^2 + v_{pz}^2 q^2}$
P7	$1 = (v_{px}^2 p^2 + v_{pz}^2 q^2)^{1/2} + \frac{v_{pz}^2 (v_{pn}^2 - v_{px}^2) p^2 q^2}{2(v_{px}^2 p^2 + v_{pz}^2 q^2)^{1/2} (v_{pn}^4 v_{px}^{-2} p^2 + v_{pz}^2 q^2)}$
P8	$1 = v_{px}^2 p^2 + v_{pz}^2 q^2 + \frac{(v_{pz}^2 - v_{sz}^2)(v_{pn}^2 - v_{px}^2) p^2 q^2}{v_{px}^2 p^2 + v_{pz}^2 q^2 - v_{sz}^2 (p^2 + q^2)}$
P9	$1 = (v_{px}^2 p^2 + v_{pz}^2 q^2)^{1/2} + \frac{(v_{pz}^2 - V_{sz}^2)(v_{pn}^2 - v_{px}^2) p^2 q^2}{2(v_{px}^2 p^2 + v_{pz}^2 q^2)^{1/2} [v_{px}^2 p^2 + v_{pz}^2 q^2 - v_{sz}^2 (p^2 + q^2)]}$
P10	$1 = V_{pz} (p^2 + q^2)^{-3/2} \times \left[(p^2 + q^2)^2 + q^2 (p^2 + q^2) + \frac{p^2}{v_{pz}^2} (v_{px}^2 p^2 + v_{pn}^2 q^2) \right]$
SV1	$2 = 2v_{sz}^2 (p^2 + q^2) + v_{px}^2 p^2 + v_{pz}^2 q^2 - \sqrt{(v_{px}^2 p^2 + v_{pz}^2 q^2)^2 + 4v_{pz}^2 (v_{sz}^2 - v_{sn}^2) p^2 q^2}$
SV2	$1 = v_{sz}^2 (p^2 + q^2) - \frac{v_{pz}^2 (v_{sz}^2 - v_{sn}^2) p^2 q^2}{v_{px}^2 p^2 + v_{pz}^2 q^2}$
SV3	$1 = v_{sz} (p^2 + q^2)^{1/2} - \frac{v_{pz}^2 (v_{sz}^2 - v_{sn}^2) p^2 q^2}{2v_{sz} (p^2 + q^2)^{1/2} (v_{px}^2 p^2 + v_{pz}^2 q^2)}$
SV4	$1 = v_{sz}^2 (p^2 + q^2) - \frac{(v_{sz}^2 - v_{sn}^2) p^2 q^2}{p^2 + q^2}$
SV5	$1 = v_{sz} (p^2 + q^2)^{1/2} - \frac{(v_{sz}^2 - v_{sn}^2) p^2 q^2}{2v_{sz} (p^2 + q^2)^{3/2}}$
SV6	$1 = v_{sz}^2 (p^2 + q^2) - \frac{v_{pz}^2 (v_{sz}^2 - v_{sn}^2) p^2 q^2}{v_{pn}^4 v_{px}^{-2} p^2 + v_{pz}^2 q^2}$
SV7	$1 = v_{sz} (p^2 + q^2)^{1/2} - \frac{v_{pz}^2 (v_{sz}^2 - v_{sn}^2) p^2 q^2}{2v_{sz} (p^2 q^2)^{1/2} (v_{pn}^4 v_{px}^{-2} p^2 + v_{pz}^2 q^2)}$
SV8	$1 = v_{sz}^2 (p^2 + q^2) - \frac{(v_{pz}^2 - v_{sz})(v_{sz}^2 - v_{sn}^2) p^2 q^2}{v_{px}^2 p^2 + v_{pz}^2 q^2 - v_{sz}^2 (p^2 + q^2)}$
SV9	$1 = v_{sz} (p^2 + q^2)^{1/2} - \frac{(v_{pz}^2 - v_{sz}^2)(v_{sz}^2 - v_{sn}^2) p^2 q^2}{2v_{sz} (p^2 + q^2)^{1/2} [(v_{px}^2 p^2 + v_{pz}^2 q^2 - v_{sz}^2 (p^2 + q^2)]}$

invariant media. If one defines the vertical two-way P-wave travel time τ_P in such media as $\tau_P = z/v_{pz}$ then $q = dt/dz = (dt/d\tau_P)(d\tau_P/dz) = r/v_{pz}$ where $r \equiv dt/d\tau_P$. Eq. (65) then becomes

$$r(p) = \sqrt{\frac{1 - v_{px}^2 p^2}{1 + (v_{pn}^2 - v_{px}^2) p^2}}. \tag{66}$$

The vertical velocity v_{pz} now no longer appears explicitly. This means that P-wave imaging can be performed using only the two parameters v_{pn} and v_{px}, as previously concluded by Alkhalifah and Tsvankin (1995). Depth conversion from τ_P to z using v_{pz} can then be postponed to a separate subsequent step. This is very useful, because v_{px} and v_{pn} can be estimated from surface seismic data, whereas v_{pz} will usually require additional borehole data to evaluate. This convenient decoupling of P-wave imaging from depth conversion has been used previously for imaging in the

presence of elliptic anisotropy with a vertical symmetry axis (ver West, 1989), and the P1 approximation extends it to the more physically realistic case of VTI. Note that the P2, P3, P6, and P7 approximations also have this same useful property, but the other P-wave phase velocity approximations given here appear not to.

The preceding discussion of phase velocity functions and dispersion relations formally holds only for homogeneous media, but can be extended to vertically stratified VTI media using essentially the same methods as are commonly used for layered isotropic media. Snell's law still holds for the phase velocities, and can be used to refract rays at each layer interface for ray shooting methods. Phase shift migration methods (Gazdag, 1978; Dubrulle, 1983) can use the anisotropic dispersion relations in the wave number domain to extrapolate waves downward, just as for the isotropic case. Based on either of these approaches, the possibility of P-wave imaging using only the two parameters v_{px} and v_{pn} for each layer can be extended from homogeneous media to layered media, with the interval vertical velocities v_{pz} again needed only for depth conversion.

For both ray shooting and for phase shift migration, it is useful to be able to express the phase velocity directly as a function of the horizontal slowness p. This can be done by expanding each dispersion relation into polynomial form, substituting $q^2=(1/v^2)-p^2$, and then multiplying the resulting expression through by the appropriate power of v^2. Solving for $v(p)$ then entails the same degree of difficulty of solving a quadratic or quartic polynomial equation as does solving the corresponding dispersion polynomial for $q(p)$. Approximation P1 is again perhaps the easiest case to solve, with Eq. (64) becoming

$$v_P^2(p)=\frac{v_{pz}^2[1+(v_{pn}^2-v_{px}^2)p^2]}{1+(v_{pz}^2-v_{px}^2)p^2+v_{pz}^2(v_{pn}^2-v_{px}^2)p^4}. \quad (67)$$

The approximate dispersion relations can also be further converted into corresponding differential wave equations. To do so, one can write the dispersion relation in expanded polynomial form, substitute $p=K_x/\omega$ and $q=K_z/\omega$, multiply through by enough powers of ω to clear the denominators, and then further substitute $K_x \rightarrow -i(\partial/\partial x)$ and $\omega \rightarrow i(\partial/\partial t)$. Alkhalifah (2000) used this approach to convert the P1 dispersion relation approximation into a fourth-order partial differential equation that could be solved numerically using a finite-difference scheme. Klie and Toro (2001) further approximated Alkhalifah's method to derive a simpler partial differential equation that was only second order in time. Klie and Toro's (2001) approximation can be shown to be equivalent to the P2 approximation given here. Converting the dispersion relations to differential equations in this manner allows one to handle lateral variations in the velocity parameters as well as vertical ones. Alkhalifah et al. (2001) have shown that even in the presence of lateral velocity variation, most P-wave imaging in VTI media can still be performed remarkably accurately using only the two parameters v_{px} and v_{pn}.

5. Group velocity approximations

For imaging in space-time coordinates it is often preferable to work with the group angle ϕ and group velocity $V(\phi)$ instead of the phase angle θ and phase velocity $v(\theta)$. In general, the group velocity and group angle can be found from the phase velocity and phase angle via the relations

$$V^2(\phi)=v^2(\theta)+\left[\frac{dv(\theta)}{d\theta}\right]^2 \quad (68)$$

and

$$\tan(\phi-\theta)=\frac{1}{v(\theta)}\frac{dv(\theta)}{d\theta}. \quad (69)$$

For the elliptic SH-wave case, one can solve explicitly in closed form for group velocity $V(\phi)$, with the resulting expression having the same elliptic form as the phase velocity Eq. (1), but with slownesses (reciprocal velocities) substituted everywhere for velocities:

$$V_{SH}^{-2}(\phi)=v_{pz}^{-2}\cos^2\phi+v_{px}^{-2}\sin^2\phi. \quad (70)$$

For exact or approximate P-wave or SV-wave phase velocities in VTI media, I know of no such simple explicit solution for group angles and velocities, so the latter must be derived numerically from the

phase angles and velocities. However, Muir and Dellinger (1985), Dellinger et al. (1993), and Harlan (1995) have all suggested using the substitution of group slownesses for phase velocities to obtain reasonable approximations for cases other than just elliptic SH waves. Dellinger and Muir (1985) pointed out that under this substitution the general Eqs. (68) and (69) defining the relations between phase and group parameters yield the equally valid and nicely symmetric relations

$$v^{-2}(\theta) = V^{-2}(\phi) + \left[\frac{\mathrm{d}V^{-1}(\phi)}{\mathrm{d}\phi}\right]^2 \tag{71}$$

and

$$\tan(\theta - \phi) = V(\phi)\frac{\mathrm{d}[V^{-1}(\phi)]}{\mathrm{d}\phi}, \tag{72}$$

which at least argues for the plausible applicability of this approximation. The obvious drawback of depending on this heuristic substitution is that quantitative error analysis is now much more difficult; the countervailing advantage is that it allows us to perform direct computations with the group angles and velocities.

Making this substitution directly into the exact phase velocity equation (Eq. (18)) does not yield viable group velocity approximations. However, transforming the P1 approximation in Eq. (40) does work reasonably well, yielding the group velocity approximation

$$2V_{\mathrm{P}}^{-2}(\phi) = V_{\mathrm{pe}}^{-2}(\phi) + \sqrt{V_{\mathrm{pe}}^{-4}(\phi) + v_{\mathrm{pz}}^{-2}(v_{\mathrm{p}n}^{-2} - v_{\mathrm{p}x}^{-2})\sin^2 2\phi}, \tag{73}$$

where I define the elliptical P-wave group velocity $V_{\mathrm{pe}}(\phi)$ by

$$V_{\mathrm{pe}}^{-2}(\phi) \equiv v_{\mathrm{p}x}^{-2}\sin^2\phi + v_{\mathrm{p}z}^{-2}\cos^2\phi. \tag{74}$$

Eq. (73) can also be shown to be identical to Eq. (6) of Zhang and Uren (2001) if the specific choice is made of $A = 2\eta$ for their free parameter A.

Dellinger et al. (1993) used a similar transformation to convert the P2 approximation in Eq. (42) into

$$V_{\mathrm{P}}^{-2}(\phi) = V_{\mathrm{pe}}^{-2}(\phi) + \frac{v_{\mathrm{p}z}^{-2}(v_{\mathrm{p}n}^{-2} - v_{\mathrm{p}x}^{-2})}{V_{\mathrm{pe}}^{-2}(\phi)}\sin^2\phi\cos^2\phi \tag{75}$$

and the SV4 approximation into

$$V_{\mathrm{SV}}^{-2}(\phi) = v_{\mathrm{s}z}^{-2} - (v_{\mathrm{s}z}^{-2} - v_{\mathrm{s}n}^{-2})\sin^2\phi\cos^2\phi. \tag{76}$$

Harlan (1995) similarly suggested converting the P4 approximation into

$$V_{\mathrm{P}}^{-2}(\phi) = V_{\mathrm{pe}}^{-2}(\phi) + (v_{\mathrm{p}n}^{-2} - v_{\mathrm{p}x}^{-2})\sin^2\phi\cos^2\phi. \tag{77}$$

This last form is also equivalent to the one used by Byun et al. (1989).

The same substitution of group slownesses for phase velocities can also be used similarly to convert the other phase velocity approximations into corresponding group velocity approximations. These group velocity approximations can also generally be derived from each other by successive approximations analogous to those used in deriving the phase velocity approximations. All these group velocity approximations are summarized in Table 4.

Note that in computing the phase velocity approximations one could make free use of Eq. (16) to interchange factors of $v_{\mathrm{p}n}^2 - v_{\mathrm{p}x}^2$ with factors of $v_{\mathrm{s}x}^2 - v_{\mathrm{s}n}^2$ as convenient. This substitution is no longer so useful for group velocities. The simple heuristic substitution of group slownesses for phase velocities into Eq. (16) is quite inaccurate; the actual corresponding relation for slownesses is instead

$$v_{\mathrm{p}n}^{-2} - v_{\mathrm{p}x}^{-2} = \frac{v_{\mathrm{s}x}^2 v_{\mathrm{s}n}^2}{v_{\mathrm{p}x}^2 v_{\mathrm{p}n}^2}(v_{\mathrm{s}x}^{-2} - v_{\mathrm{s}n}^{-2}). \tag{78}$$

Thus one could actually derive two quite different sets of group velocity approximations, one using factors of $v_{\mathrm{p}n}^{-2} - v_{\mathrm{p}x}^{-2}$ and the other using $v_{\mathrm{s}x}^{-2} - v_{\mathrm{s}n}^{-2}$. Thus, as a simple example, one could

Table 4
Group velocity approximations

P1	$2V_P^{-2}(\phi) = V_{pe}^{-2}(\phi) + \sqrt{V_{pe}^{-4}(\phi) + v_{pz}^{-2}(v_{pn}^{-2} - v_{px}^{-2})\sin^2 2\phi}$
P2	$V_P^{-2}(\phi) = V_{pe}^{-2}(\phi) + \frac{v_{pz}^{-2}(v_{pn}^{-2} - v_{px}^{-2})}{V_{pe}^{-2}(\phi)}\sin^2\phi\cos^2\phi$
P3	$V_P^{-1}(\phi) = V_{pe}^{-1}(\phi) + \frac{v_{pz}^{-2}(v_{pn}^{-2} - v_{px}^{-2})}{2V_{pe}^{-3}(\phi)}\sin^2\phi\cos^2\phi$
P4	$V_P^{-2}(\phi) = V_{pe}^{-2}(\phi) + (v_{pn}^{-2} - v_{px}^{-2})\sin^2\phi\cos^2\phi$
P5	$V_P^{-1}(\phi) = V_{pe}^{-1}(\phi) + \frac{(v_{pn}^{-2} - v_{px}^{-2})}{2V_{pe}^{-1}(\phi)}\sin^2\phi\cos^2\phi$
P6	$V_P^{-2}(\phi) = V_{pe}^{-2}(\phi) + \frac{v_{pz}^{-2}(v_{pn}^{-2} - v_{px}^{-2})}{v_{pz}^{-2}\cos^2\phi + v_{pn}^{-4}v_{px}^{2}\sin^2\phi}\times \sin^2\phi\cos^2\phi$
P7	$V_P^{-1}(\phi) = V_{pe}^{-1}(\phi) + \frac{v_{pz}^{-2}(v_{pn}^{-2} - v_{px}^{-2})}{2V_{pe}^{-1}(\phi)(v_{pz}^{-2}\cos^2\phi + v_{pn}^{-4}v_{px}^{2}\sin^2\phi}\times \sin^2\phi\cos^2\phi$
P8	$V_P^{-2}(\phi) = V_{pe}^{-2}(\phi) + \frac{(v_{pz}^{-2} - v_{sz}^{-2})(v_{pn}^{-2} - v_{px}^{-2})}{V_{pe}^{-2}(\phi) - v_{sz}^{-2}}\sin^2\phi\cos^2\phi$
P9	$V_P^{-1}(\phi) = V_{pe}^{-1}(\phi) + \frac{(v_{pz}^{-2} - v_{sz}^{-2})(v_{pn}^{-2} - v_{px}^{-2})}{2V_{pe}^{-1}(\phi)[V_{pe}^{-2}(\phi) - v_{sz}^{-2}}\sin^2\phi\cos^2\phi$
P10	$2V_P^{-1}(\phi) = v_{pz}^{-1}[1 + \cos^2\phi + v_{pz}^{2}v_{pn}^{-2}\sin^2\phi\cos^2\phi + v_{pz}^{2}v_{px}^{-2}\sin^4\phi]$
SV1	$2V_{SV}^{-2}(\phi) = 2v_{sz}^{-2} + V_{pe}^{-2}(\phi) - \sqrt{V_{pe}^{-4}(\phi) + v_{pz}^{-2}(v_{sz}^{-2} - v_{sn}^{-2})\sin^2 2\phi}$
SV2	$V_{SV}^{-2}(\phi) = v_{sz}^{-2} - \frac{v_{pz}^{-2}(v_{sz}^{-2} - v_{sn}^{-2})}{V_{pe}^{-2}(\phi)}\sin^2\phi\cos^2\phi$
SV3	$V_{SV}^{-1}(\phi) = v_{sz}^{-1} - \frac{v_{pz}^{-2}(v_{sz}^{-2} - v_{sn}^{-2})}{2v_{sz}^{-1}V_{pe}^{-2}(\phi)}\sin^2\phi\cos^2\phi$

Table 4 (*continued*)

SV4	$V_{SV}^{-2}(\phi) = v_{sz}^{-2} - (v_{sz}^{-2} - v_{sn}^{-2})\sin^2\phi\cos^2\phi$
SV5	$V_{SV}^{-1}(\phi) = v_{sz}^{-1} - \frac{(v_{sz}^{-2} - v_{sn}^{-2})}{2v_{sz}^{-1}}\sin^2\phi\cos^2\phi$
SV6	$V_{SV}^{-2}(\phi) = v_{sz}^{-2} - \frac{v_{pz}^{-2}(v_{sz}^{-2} - v_{sn}^{-2})}{v_{pz}^{-2}\cos^2\phi + v_{pn}^{-4}v_{px}^{2}\sin^2\phi}\sin^2\phi\cos^2\phi$
SV7	$V_{SV}^{-1}(\phi) = v_{sz}^{-1} - \frac{v_{pz}^{-2}(v_{sz}^{-2} - v_{sn}^{-2})}{2v_{sz}^{-1}(v_{pz}^{-2}\cos^2\phi + v_{pn}^{-4}v_{px}^{2}\sin^2\phi)}\times \sin^2\phi\cos^2\phi$
SV8	$V_{SV}^{-2}(\phi) = v_{sz}^{-2} - \frac{(v_{pz}^{-2} - v_{sz}^{-2})(v_{sz}^{-2} - v_{sn}^{-2})}{v_{pe}^{-2}(\phi) - v_{sz}^{-2}}\sin^2\phi\cos^2\phi$
SV9	$V_{SV}^{-1}(\phi) = v_{sz}^{-1} - \frac{(v_{pz}^{-2} - v_{sz}^{-2})(v_{sz}^{-2} - v_{sn}^{-2})}{2v_{sz}^{-1}(V_{pe}^{-2}(\phi) - v_{sz}^{-2})}\sin^2\phi\cos^2\phi$

write the P4 phase velocity approximation in Eq. (45) equally well as

$$v_P(\theta) = v_{pe}(\theta) + (v_{sx}^2 - v_{sn}^2)\sin^2\theta\cos^2\theta. \quad (79)$$

Applying the heuristic substitution of group slowness for phase velocities to these two equivalent phase velocity expressions, however, results in two distinct possible group velocity approximations:

$$V_P^{-2}(\phi) = V_{pe}^{-2}(\phi) + (v_{pn}^{-2} - v_{px}^{-2})\sin^2\phi\cos^2\phi \quad (80)$$

or

$$V_P^{-2}(\phi) = V_{pe}^{-2}(\phi) + (v_{sx}^{-2} - v_{sn}^{-2})\sin^2\phi\cos^2\phi. \quad (81)$$

From Eq. (78) it follows that these two group velocity approximations will not be equivalent. Based simply on empirical testing of comparative accuracy, I have used the first choice in the P-wave group velocity approximations, writing them in terms of $v_{pn}^{-2} - v_{px}^{-2}$ factors, and the second choice in the SV-wave group velocity approximations, writing them instead in terms of $v_{sx}^{-2} - v_{sn}^{-2}$ factors.

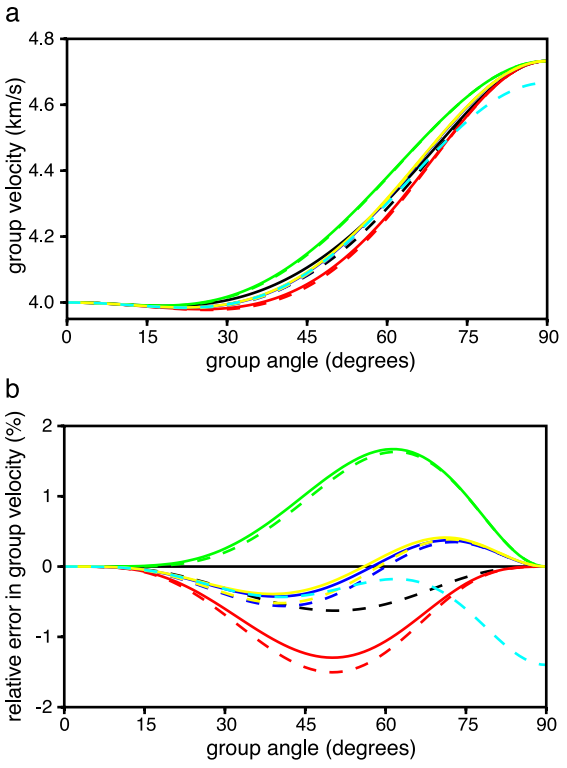

Fig. 5. P-wave group velocity approximations. The upper plot shows various P-wave group velocity approximations, and the lower plot shows the relative errors compared to the exact P-wave group velocity. The black line is the exact P-wave group velocity for $v_{pz}=4$ km/s, $\epsilon=0.2$, and $\delta=-0.05$, and $v_{sz}=1$ km/s. Approximation P1 is the black dashed line, P2 is solid red, P3 is dashed red, P4 is solid blue, P5 is dashed blue, P6 is solid green, P7 is dashed green, P8 is solid yellow, P9 is dashed yellow, and P10 is dashed light blue.

Fig. 5 compares the different P-wave group velocity approximations using again the parameters $v_{pz}=4$ km/s, $v_{sz}=1$ km/s, $\epsilon=0.2$, and $\delta=-0.05$. The upper plot compares the different group velocity approximations, and the second shows the errors relative to the exact group velocity, computed now numerically from the exact phase velocity. The color coding is the same as in Fig. 3: the solid black line represents the exact P-wave group velocity, approximation P1 is the black dashed line, P2 is solid red, P3 is dashed red, P4 is solid blue, P5 is dashed blue, P6 is solid green, P7 is dashed green, P8 is solid yellow, P9 is dashed yellow, and P10 is dashed light blue. Like the phase velocities in Fig. 3, the group velocity approximations in Fig. 5 are generally quite accurate, with a maximum error of less than 2%. The patterns of error for the group velocities are quite different from those for the phase velocities, however, so one cannot just assume that the best phase velocity approximation will automatically correspond to the best group velocity approximation under the heuristic substitution used here. In contrast, group velocities computed numerically by applying Eqs. (68) and (69) to the various phase velocity approximations will, of course, mirror the error patterns of the corresponding phase velocities approximations.

Fig. 6 similarly compares the different SV-wave group velocity approximations, again for the same model parameters. The color coding is the same as in

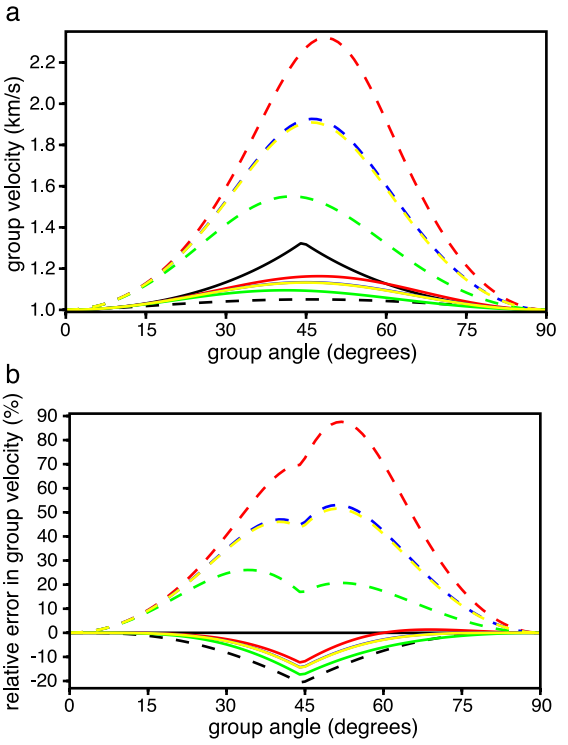

Fig. 6. SV-wave group velocity approximations. The upper plot shows various SV-wave group velocity approximations, and the lower plot shows the relative errors compared to the exact SV-wave group velocity. The black line is the exact SV-wave group velocity for $v_{pz}=4$ km/s, $\epsilon=0.2$, and $\delta=-0.05$, and $v_{sz}=1$ km/s. Approximation SV1 is the black dashed line, SV2 is solid red, SV3 is dashed red, SV4 is solid blue, SV5 is dashed blue, SV6 is solid green, SV7 is dashed green, SV8 is solid yellow, and SV9 is dashed yellow.

Fig. 4: the solid black line represents the exact SV-wave group velocity, approximation SV1 is the black dashed line, SV2 is solid red, SV3 is dashed red, SV4 is solid blue, SV5 is dashed blue, SV6 is solid green, SV7 is dashed green, SV8 is solid yellow, and SV9 is dashed yellow. The exact group velocity curve now actually is triplicating, with only the minimum group velocity segments of the curve shown in the plot. The limitations of the approximations made here become apparent in this figure; none of them fit well near the triplication. The linearized $V_{SV}(\phi)$ approximations (colored dashed lines) all seriously over estimate the actual group velocity. The various $v_{SV}^2(\phi)$ approximations (colored solid lines) fit reasonably well near the vertical and horizontal axes, but underestimate the group velocity near the triplication. The SV1 approximation, which worked very well for the SV-wave phase velocity, does not fit nearly as well for SV-wave group velocities. The relative errors of all the SV-wave group velocity approximations are substantially worse than for the phase velocities or for the P-wave group velocities.

6. Travel time approximations

Just as the phase velocity approximations can be converted into dispersion relations, the group velocity approximations can be converted into travel time or moveout equations. These are particularly useful for space-time imaging methods.

Consider a ray segment travelling at the (group) angle ϕ, traversing a horizontal distance x, a vertical distance z, and a time increment t. One then has

$$\sin\phi = \frac{x}{V(\phi)t} \tag{82}$$

$$\cos\phi = \frac{z}{V(\phi)t}. \tag{83}$$

Substituting these expressions into the group velocity approximations gives equivalent travel time equations. For example, with these substitutions the P1 group velocity approximation yields the travel time equation

$$t_P^4 - (v_{px}^{-2}x^2 + v_{pz}^2 z^2)t^2 - v_{pz}^{-2}(v_{pn}^{-2} - v_{px}^{-2})x^2 z^2 = 0 \tag{84}$$

or

$$2t_P^2 = t_{pe}^2 + \sqrt{t_{pe}^4 + 4v_{pz}^{-2}(v_{pn}^{-2} - v_{px}^{-2})x^2 z^2}, \tag{85}$$

where I define the elliptic travel time t_{pe} by

$$t_{pe}^2 \equiv \frac{x^2}{v_{px}^2} + \frac{z^2}{v_{pz}^2}. \tag{86}$$

The other group velocity approximations can similarly be converted into travel time approximations; the results are summarized in Table 5. In the SV-wave travel time approximations listed there, I have used the shorthand definition of the circular shear velocity

$$t_{sc}^2 \equiv \frac{x^2 + z^2}{v_{sz}^2}, \tag{87}$$

in analogy with the elliptic P-wave travel time t_{pe}.

The P1 approximation allows a convenient decoupling of imaging and depth conversion in the space-time domain, just as was possible for the dispersion relation in the frequency-wave number domain. Replacing the depth z with the vertical travel time $\tau_P = z/v_{pz}$ converts the P1 approximation into

$$2t_P^2 = \tau_P^2 + \frac{x^2}{v_{px}^2} + \sqrt{\left(\tau_P^2 + \frac{x^2}{v_{px}^2}\right)^2 + 4(v_{pn}^{-2} - v_{px}^{-2})x^2\tau_P^2}. \tag{88}$$

The vertical velocity v_{pz} has again disappeared, allowing complete specification of P-wave travel times using only v_{pn} and v_{px}. As with the dispersion relations, this useful decoupling of imaging from depth conversion again appears to hold also for the P2, P3, P6, and P7 approximations, but not for the other P-wave approximations.

The travel time approximation P6 in Table 5 is written in the form of a perturbation away from the elliptical travel time t_{pe}, but it can also be recast in the equivalent form

$$t_P^2 = \tau_P^2 + \frac{x^2}{v_{pn}^2} + \frac{(v_{pn}^2 - v_{px}^2)x^4}{v_{pn}^2(v_{pn}^4\tau_P^2 + v_{px}^2x^2)}, \tag{89}$$

using again the vertical P-wave travel time $\tau_P = z/v_{pz}$. This is the travel time approximation suggested by

Table 5
Travel time approximations

P1	$2t_P^2 = t_{pe}^2 + \sqrt{t_{pe}^4 + 4v_{pz}^{-2}(v_{pn}^{-2} - v_{px}^{-2})x^2z^2}$
P2	$t_P^2 = t_{pe}^2 + \frac{v_{pz}^{-2}(v_{pn}^{-2} - v_{px}^{-2})x^2z^2}{t_{pe}^2}$
P3	$t_P = t_{pe} + \frac{v_{pz}^{-2}(v_{pn}^{-2} - v_{px}^{-2})x^2z^2}{2t_{pe}^3}$
P4	$t_P^2 = t_{pe}^2 + \frac{v_{sz}^{-2}(v_{pn}^{-2} - v_{px}^{-2})x^2z^2}{t_{sc}^2}$
P5	$t_P = t_{pe} + \frac{v_{sz}^{-2}(v_{pn}^{-2} - v_{px}^{-2})x^2z^2}{2t_{pe}t_{sc}^2}$
P6	$t_P^2 = t_{pe}^2 + \frac{v_{pz}^{-2}(v_{pn}^{-2} - v_{px}^{-2})x^2z^2}{v_{pz}^{-2}z^2 + v_{px}^2v_{pn}^{-4}x^2}$
P7	$t_P = t_{pe} + \frac{(v_{pn}^{-2} - v_{px}^{-2})x^2z^2}{2t_{pe}(v_{pz}^{-2}z^2 + v_{px}^2v_{pn}^{-4}x^2)}$
P8	$t_P^2 = t_{pe}^2 + \frac{(v_{pz}^{-2} - v_{sz}^{-2})(v_{pn}^{-2} - v_{px}^{-2})x^2z^2}{t_{pe}^2 - t_{sc}^2}$
P9	$t_P = t_{pe} + \frac{(v_{pz}^{-2} - v_{sz}^{-2})(v_{pn}^{-2} - v_{px}^{-2})x^2z^2}{2t_{pe}(t_{pe}^2 - t_{sc}^2)}$
P10	$t_P = v_{pz}^{-1}v_{sz}t_{sc}\left[1 + \frac{z^2}{v_{sz}^2t_{sc}^2} + \frac{v_{pz}^2x^2}{v_{sz}^4t_{sc}^4}\left(\frac{z^2}{v_{pn}^2} + \frac{x^2}{v_{px}^2}\right)\right]$
SV1	$2t_{SV}^2 = 2t_{sc}^2 + t_{pe}^2 - \sqrt{t_{pe}^4 + 4v_{pz}^{-2}(v_{sz}^{-2} - v_{sn}^{-2})x^2z^2}$
SV2	$t_{SV}^2 = t_{sc}^2 - \frac{v_{pz}^{-2}(v_{sz}^{-2} - v_{sn}^{-2})x^2z^2}{t_{pe}^2}$
SV3	$t_{SV} = t_{sc} - \frac{v_{pz}^{-2}(v_{sz}^{-2} - v_{sn}^{-2})x^2z^2}{2t_{sc}t_{pe}^2}$
SV4	$t_{SV}^2 = t_{sc}^2 - \frac{v_{sz}^{-2}(v_{sz}^{-2} - v_{sn}^{-2})x^2z^2}{t_{sc}^2}$
SV5	$t_{SV} = t_{sc} - \frac{v_{sz}^{-2}(v_{sz}^{-2} - v_{sn}^{-2})x^2z^2}{2t_{sc}^3}$
SV6	$t_{SV}^2 = t_{sc}^2 - \frac{v_{pz}^{-2}(v_{sz}^{-2} - v_{sn}^{-2})x^2z^2}{v_{pz}^{-2}z^2 + v_{px}^2v_{pn}^{-4}x^2}$
SV7	$t_{SV} = t_{sc} - \frac{(v_{sz}^{-2} - v_{sn}^{-2})x^2z^2}{2t_{sc}(v_{pz}^{-2}z^2 + v_{px}^2v_{pn}^{-4}x^2)}$
SV8	$t_{SV}^2 = t_{sc}^2 - \frac{(v_{pz}^{-2} - v_{sz}^{-2})(v_{sz}^{-2} - v_{sn}^{-2})x^2z^2}{t_{pe}^2 - t_{sc}^2}$
SV9	$t_{SV} = t_{sc} - \frac{(v_{pz}^{-2} - v_{sz}^{-2})(v_{sz}^{-2} - v_{sn}^{-2})x^2z^2}{2t_{sc}(t_{pe}^2 - t_{sc}^2)}$

Tsvankin and Thomsen (1994), converted into the form of Eq. 4.29 of Tsvankin (2001). Note that the travel time approximation P2, based on the group velocity approximation of Dellinger et al. (1993), can similarly be rewritten as

$$t_P^2 = \tau_P^2 + \frac{x^2}{v_{pn}^2} + \frac{(v_{pn}^2 - v_{px}^2)x^4}{v_{pn}^2v_{px}^2(v_{pn}^2\tau_P^2 + x^2)}, \tag{90}$$

which differs from the Tsvankin–Thomsen approximation in Eq. (89) by only the substitution of one factor of v_{px}^2 for v_{pn}^2 in the denominator of the third term. These two approximations, derived originally by very different reasoning, are thus very similar but not quite identical.

These approximate travel time equations are formally valid only for homogenous media. For inhomogeneous media they can be applied for ray segments short enough that spatially varying media parameters can be approximated as being locally homogeneous. Also, as in the common use of hyperbolic moveout approximations for conventional velocity analysis in layered isotropic media, these various anisotropic travel time equations can also be used to approximate moveout in vertically inhomogenous VTI media. In such applications to layered media, the media parameters such as v_{px} and v_{pn} that appear in the travel time equations are now interpreted as particular vertical averages of the actual physical parameters in each

layer (Tsvankin and Thomsen, 1994;Alkhalifah and Tsvankin, 1995; Tsvankin, 2001).

7. Discussion and Conclusions

Because phase velocities in VTI media have a closed form analytic solution, they are easier to approximate well than are the corresponding group velocities. With a good choice of parametrization, P-wave phase velocities become nearly independent of the shear velocity v_{sz}. The key to deriving such a parametrization is using a factorization of the form given in Eq. (24). Any choice of v_{p1} in this factorization such that $v_{pmin}^2 \le v_{p1}^2 \le v_{pmax}^2$ and $v_{pmin}^2 \le v_{p2}^2 \le v_{pmax}^2$ will generally allow one to eliminate v_{sz}. The approximation made then in dropping v_{sz} can be quantified and does not require recourse to arbitrarily declaring it to just be zero.

The particular choice of $v_{p1} = v_{pz}$ and $v_{p2} = v_{pn}$ works well, and leads to several other previously published approximations. Most of these different approximations will usually be adequately accurate, so in practice a choice between them might be made based on factors such as the possible desire to also eliminate v_{pz} for use in time imaging, the ease of solving the dispersion relation for $q(p)$ or $v(p)$, or the importance of having an approximation that is linear in its parameters.

SV-wave anisotropy is closely coupled to P-wave anellipticity, and each P-wave phase velocity approximation leads naturally to a corresponding SV-wave phase velocity approximation. Roughly speaking, P-wave phase velocities are a perturbation away from elliptic, and SV-wave phase velocities are the same perturbation away from circular, but with the opposite sign. However, because the shear velocities are smaller than the P-wave velocities, the relative errors in the SV-wave approximations tend to be larger than the relative errors of the corresponding P-wave approximations.

Because there is no exact closed form expression for P-wave and SV-wave group velocities in VTI media, it is more difficult to derive good approximations for them. However, a simple heuristic substitution of group slownesses for phase velocities into the different phase velocity approximations does generally yield plausible group velocity and travel time approximations. For P waves, the resulting group velocity approximations are usually of comparable accuracy to the corresponding phase velocity approximations. For SV waves, this heuristic substitution does not always work as well, and the accuracy of the resulting SV-wave group velocity approximations can be poor. This is not entirely surprising, because for SV-wave group velocities one is trying to approximate a rapidly changing and even multivalued function with simpler, smoother functions.

Acknowledgements

I thank Tariq Alkhalifah, Dennis Corrigan, Joe Dellinger, Jim Gaiser, Bill Harlan, and Ilya Tsvankin for many useful and enlightening discussions. I also thank Claudia Vanelle and Alexandre Stopin for excellent and thorough reviews that greatly improved this paper. All remaining errors and misconceptions here are my responsibility alone, of course.

References

Alkhalifah, T., 1998. Acoustic approximations for processing in transversely isotropic media. Geophysics 63, 623–631.

Alkhalifah, T., 2000. An acoustic wave equation for anisotropic media. Geophysics 65, 1239–1250.

Alkhalifah, T., Tsvankin, I., 1995. Velocity analysis for transversely isotropic media. Geophysics 60, 1550–1566.

Alkhalifah, T., Fomel, S., Biondi, B., 2001. The space-time domain: theory and modelling for anisotropic media. Geophysical Journal International 144, 105–113.

Auld, B.A., 1990. Acoustic Fields and Waves in Solids, vols. 1 and 2. Robert E. Krieger Publishing, Malabar, FL.

Byun, B.S., Corrigan, D., Gaiser, J.E., 1989. Anisotropic velocity analysis for lithology discrimination. Geophysics 54, 1564–1574.

Claerbout, J.F., 1984. Imaging the Earth's Interior Blackwell, Palo Alto.

Dellinger, J., Muir, F., 1985. Two domains of anisotropy. Stanford Exploration Project Report 44, 59–62.

Dellinger, J., Muir, F., Karrenbach, M., 1993. Anelliptic approximations for TI media. Journal of Seismic Exploration 2, 23–40.

Dubrulle, A.A., 1983. Numerical methods for the migration of constant-offset sections in homogeneous and horizontally layered media. Geophysics 48, 1195–1203.

Gaiser, J.E., 1989. Transverse isotropic velocity estimates from slowness and displacement measurements. PhD dissertation, University of Texas at Dallas.

Gazdag, J., 1978. Wave equation migration with the phase-shift method. Geophysics 43, 1342–1351.

Harlan, W., 1995. Flexible seismic traveltime tomography ap-

plied to diving waves. Stanford Exploration Project Report 89, 145–164.

Klie, H., Toro, W., 2001. A new acoustic wave equation for modeling in anisotropic media. 71st Annual International Meeting, Society of Exploration Geophysicists, Expanded Abstracts, 1171–1173.

Michelena, R.J., 1993. Anisotropic traveltime tomography. PhD dissertation, Stanford University.

Muir, F., Dellinger, J., 1985. A practical anisotropic system. Stanford Exploration Project Report 44, 55–58.

Schoenberg, M.A., de Hoop, M.V., 2000. Approximate dispersion relations for qP–qSV-waves in transversely isotropic media. Geophysics 65, 919–933.

Stolt, R.H., 1978. Migration by Fourier transform. Geophysics 43, 23–48.

Stopin, A., 2001. Comparison of $v(\theta)$ equations in TI medium. 9th International Workshop on Seismic Anisotropy.

Thomsen, L., 1986. Weak elastic anisotropy. Geophysics 51, 1954–1966.

Tsvankin, I., 2001. Seismic signatures and analysis of reflection data in anisotropic media Pergamon, Oxford.

Tsvankin, I., Thomsen, L., 1994. Nonhyperbolic reflection moveout in anisotropic media. Geophysics 59, 1290–1304.

ver West, B.J., 1989. Seismic migration in elliptically anisotropic media. Geophysical Prospecting 37, 149–166.

Zhang, F., Uren, N., 2001. Approximate explicit ray velocity functions and travel times for P-waves in TI media. 71st Annual International Meeting, Society of Exploration Geophysicists, Expanded Abstracts, 106–109.